

DYNAMICS OF THE FORMATION OF A GAS SUSPENSION BEHIND A SHOCK WAVE
SLIDING OVER THE SURFACE OF A LOOSE MATERIAL

V. M. Boiko and A. N. Napyrin

In regard to the study of explosions occurring during the commercial processing and transport of powdered materials, it is important to examine the mechanism and dynamics of formation of gas suspensions behind shock waves (SW) sliding over the gas-powder interface [1]. Only isolated studies [2-7] have been made of this question, these investigations having been analyzed in [1]. According to [1], there is currently no common approach to description of the process of mixture formation behind shock waves, and the available empirical data is insufficient to construct a realistic picture of this phenomenon. Thus, at the current stage, it is necessary to first of all set up systematic experimental studies within a broad range of gas and particle parameters with the use of diagnostic methods that will permit recording of the process with a high spatial and temporal resolution.

The present article reports certain results of an experimental study of the dynamic behavior of different powdered materials ($d > 50 \mu\text{m}$, $\rho = 1.2\text{-}8.6 \text{ g/cm}^3$) behind the front of a traveling shock wave ($M = 2\text{-}3$, $p = 1 \text{ atm}$). The results were obtained by the method of multiframe shadow laser visualization.

1. The tests were conducted on a unit [7] consisting of a shock tube with a channel having a rectangular cross section $38 \times 56 \text{ mm}$ and a length of 4.5 m , diagnostic equipment, and control and synchronization systems. A layer of powder was placed in a tray with an area of 20×200 and a depth of 2 mm . The natural charge of powder was smoothed out and packed so that the roughness of its surface was only slightly greater than the size of the particles.

The dynamics of the formation of the two-phase medium was observed by means of a high-speed system for multiframe laser shadow visualization. Here, the exposure (about 30 nsec), the number of frames, and the time intervals between frames Δt were established by the laser stroboscopic light source [8]. The frames were separated spatially by a ZhFR-3 high-speed slave photorecorder. The size of the frames was $24 \times 10 \text{ mm}$, while the spatial resolution was about $50 \mu\text{m}$.

The synchronization system ensured the necessary sequence in the startup of individual elements of the shock tube and diagnostic equipment, which in turn permitted accurate generation of the counting pulses relative to the moment of passage of the SW in the test region.

In each test we recorded a series of 15-20 frames reflecting the dynamics of the process in question during a period of time $t \sim 600\text{-}800 \mu\text{sec}$. The duration of the constant parameters of the flow behind the SW front was at least $700 \mu\text{sec}$.

2. Previous studies [2-4] showed that the process of mixture formation is very heavily influenced by the projection of the front of the charge over the surface of the wall. To minimize this effect, we arranged the powder in the tray in such a way that the surface of the charge was at the same level as the surface of the lower wall of the shock tube. The tests showed that the disturbance of the gas flow by the edges of the tray was insignificant and had no appreciable effect on the dynamics of particle ascent.

Figure 1 shows a series of photographs illustrating the dynamics of ascent of spherical particles of organic glass with a diameter $d = 200\text{-}250 \mu\text{m}$ (density $\rho = 1.2 \text{ g/cm}^3$) behind a transmitted wave sliding along the charge of powder. The magnification of the optical system and the time interval between frames were chosen so that the distance traveled by the wave front during the period between two successive exposures was no greater than the dimensions of the frame (the successive positions of the wave front, moving from right to left, are visible in frames 1 and 2). This made it possible to continuously monitor the dynamics of the layer of loose material. The region of observation was located 150 mm downflow from the front

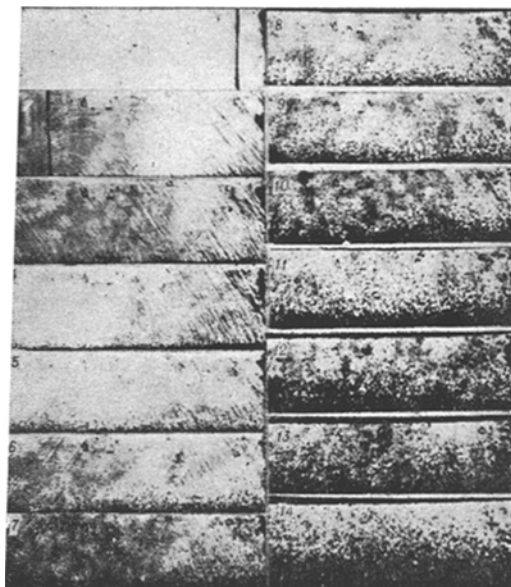


Fig. 1. Series of shadowgraphs illustrating the dynamics of the formation of a two-phase mixture behind a shock wave sliding over a gas-particle surface: $M = 2.7$, $p = 1$ atm, $\Delta t = 40$ μ sec.

of the tray. The initial state of the charge surface is shown in frame 1. In later frames, the initial position of the phase boundary is indicated by the light line.

It is evident from Fig. 1 that the following characteristic changes occur in the interaction with the SW: an increase in the roughness of the charge surface and a simultaneous increase in the thickness of the charge; the detachment of individual particles from the surface of the layer and their entrainment by the gas flow. The presence of particles suspended in the flow becomes noticeable after 70-80 μ sec (frames 3 and 4). From this time onward, a two-phase layer of increasing thickness is formed over the surface of the charge.

Photographs similar to those in Fig. 1 can be used to determine the character of the change in the concentration of the disperse phase in a given region of the channel at any moment of time. It is obvious that when measuring the thickness of the two-phase layer, the criterion chosen to determine the upper boundary of this layer is of fundamental importance. In our tests, i.e., with the use of the shadow method of recording, it was simplest to fix two parameters: the maximum height of ascent of individual particles h_+ , and the height of the upper boundary of the "solid" (optically opaque) layer of powder h_- .

Let us evaluate the volumetric concentration of the disperse phase at the level h_- . We will suppose that h_- corresponds to the height above which no particle images are superimposed, i.e., to a situation whereby no more than one particle is located in the volume bounded by the cross section of a particle and the width of the charge l , $\frac{\pi}{6} d^3 \varphi \left(\frac{\pi}{4} d^2 l \right) \leq 1$. Under these experimental conditions, $l \sim 20$ mm and $d = 200-250$ μ m, which corresponded to a value of $\varphi \sim 1\%$.

Figure 2 shows the relations $h_+(t)$ and $h_-(t)$ in tests involving the interaction of an SW with layers of spherical particles of organic glass and bronze ($\rho = 8.6$ g/cm³). Figure 3 shows the relations $h_-(t)$ for particles of organic glass with $d = 200-250$ μ m and different SW intensities. It follows from the data that the rate of ascent of the dispersed phase depends on the dynamic head of the gas (u , ρ_g) and the inertial properties of the particles (d , ρ) and increases with an increase in u and ρ_g and a decrease in d and ρ .

Let us address certain considerations in regard to the mechanism of ascent of the disperse phase under the given experimental conditions, i.e., with the use of sufficiently coarse spherical particles ($d > 50-100$ μ m). Special tests were conducted to study the interaction of an SW with "single" particles located on the polished surface of the lower wall of the shock tube. These tests showed that a single particle ($d > 50$ μ m) moves over the surface and is not lifted upward until it collides with some obstacle, such as a wire placed on the surface of the wall for this purpose. No particle lifting was also seen in tests in which single particles were initially located behind an obstacle which was 10-20 times higher than the particle size and which produced turbulence in the gas flow. These findings indicate the fundamental role of collision in lifting of the disperse phase. Thus, particles located on a "smooth" surface can evidently be made to ascend only when they are in a group of similar particles, i.e., when they collide with each other.

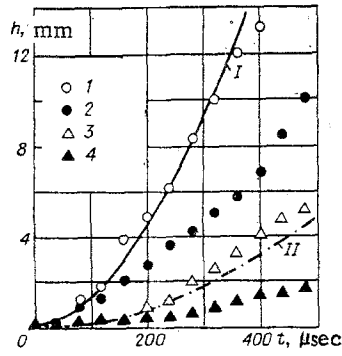


Fig. 2

Fig. 2. Height of ascent of particles above the interface in relation to the time of interaction with the SW: $M = 2.7$; $p = 1$ atm; $d = 200-250$. 1, 2) $\rho = 1.2$ g/cm³; 3, 4) $\rho = 8.6$ g/cm³; 1, 3) maximum height h_+ ; 2, 4) height h_- , corresponding to $\varphi \sim 1\%$.

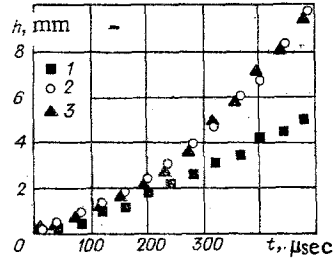


Fig. 3

Fig. 3. The relation $h_-(t)$ with different shock-wave intensities: $d = 200-250$ μ m; $\rho = 1.2$ g/cm³. 1) $M = 2.1$, $p = 1$ atm; 2) $M = 2.7$, $p = 1$ atm; 3) $M = 3.3$, $p = 0.5$ atm.

In our opinion, this situation also exists in the interaction of a slip flow with the surface of a sufficiently densely compacted layer of powder. Particles located on the surface begin to move under the influence of aerodynamic resistance, continuously colliding with each other. This leads to the development of "roughnesses" on the surface of the layer, loosening of the layer, an increase in the thickness of the latter, lifting of particles, and the formation of a two-phase layer. The concentration of the disperse phase in the two-phase layer decreases toward the upper boundary.

Photographs of the two-phase layer obtained by the laser "knife" method [9] show (Fig. 4) that, in the optically transparent region of the two-phase layer (under the conditions of the tests, $\varphi < 1\%$), the particle trajectories do not intersect. It follows from this that collision occurs mainly in the region adjacent to the surface of the charge, where $\varphi > 1\%$.

The elastic impact of a particle moving translationally against an obstacle not only changes its initial momentum but also gives it an angular velocity ω , i.e., the vertical component of the velocity of the particle responsible for its ascent may be the result both of elastic reflection and the Magnus force. Let us evaluate the contribution of each of these two factors to the dynamics of particle ascent.

With allowance for the lateral force, we write the equation of motion of the particle in the form [10]

$$\frac{d\vec{v}}{dt} = 2 \frac{\rho_g}{\rho} [\omega \vec{V}] - \frac{3}{4} \frac{C_d \rho_g}{d \rho} |\vec{V}| \vec{V}, \quad \vec{V} = \vec{v} - \vec{u}, \quad (1)$$

where ρ_g is the density of the gas; C_d is the resistance coefficient; \vec{v} and \vec{u} are the velocity vectors of the particle and gas. Let us examine the motion of the particle in the plane x, y , assuming that $\omega_x = \omega_y = 0$, $\omega_z = \omega$, $u_x = u_0$ (where $u_0 = \text{const}$), $u_y = 0$. Projecting Eq. (1) on the coordinate axes, we obtain

$$\frac{dv_x}{dt} = 2 \frac{\rho_g}{\rho} \omega v_y - \frac{3}{4} \frac{C_d \rho_g}{d \rho} |v_x - u_0| (v_x - u_0), \quad (2)$$

$$\frac{dv_y}{dt} = -2 \frac{\rho_g}{\rho} \omega (v_x - u_0) - \frac{3}{4} \frac{C_d \rho_g}{d \rho} v_y^2. \quad (3)$$

We will assume that the particle was not rotated before impact and that slip of the particle ceased as a result of the impact. Then, following [10], it is not hard to show that $\omega \leq 1.5v_0/d$, where v_0 is the translational velocity of the particle at the moment of impact. Limiting ourselves to the case $\omega = 1.5v_0/d$, we change (2) and (3) to the form

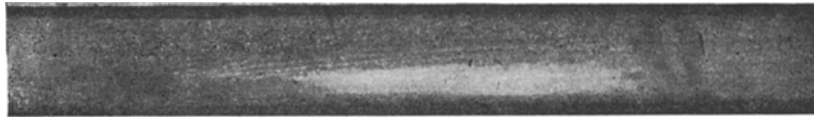


Fig. 4. Particle trajectories in the two-phase layer. The trajectories were obtained by the laser "knife" method.

$$\frac{dv_x}{dt} = \frac{1}{\tau} \frac{(u_0 - v_x) |u_0 - v_x|}{u_0} (1 + m), \quad (4)$$

$$\frac{dv_y}{dt} = \frac{1}{\tau} \frac{4v_0 (u_0 - v_x)}{C_d u_0} (1 - n), \quad (5)$$

where $\tau = \frac{4}{3} \frac{\rho d}{\rho_g C_d u_0}$ is the characteristic time of velocity relaxation,

$$m = \frac{4v_0 v_y}{C_d (u_0 - v_x)^2}, \quad n = \frac{C_d v_y^2}{4v_0 (u_0 - v_x)}. \quad (6)$$

During the initial stage of motion, $v_x \ll u_0$, $v_y \ll u_0$, $v_0 < u_0$, $C_d \sim 1$. Thus, $m \ll 1$, $n \ll 1$, and in a first approximation they can be ignored, i.e.,

$$\frac{dv_x}{dt} = \frac{1}{\tau} \frac{(u_0 - v_x)^2}{u_0} \quad (7)$$

$$\frac{dv_y}{dt} = \frac{1}{\tau} \frac{4v_0 (u_0 - v_x)}{C_d u_0} \quad (8)$$

We use (7) and (8) to obtain an expression for the rate of ascent of the particles under the influence of the Magnus force

$$v_y(t) = b \ln(1 + t/\tau), \quad (9)$$

$$b = \frac{4v_0}{C_d} = \frac{8}{3} \frac{\omega d}{C_d}. \quad (10)$$

Let us find the conditions of applicability of approximation (7), (8). We assume that $m < k$, $n < k$, where k is a constant. Then from (6) we obtain

$$v_y / (u_0 - v_x) \leq k^{2/3}. \quad (11)$$

It follows from (7) that $u_0 - v_x = u_0 / (1 + t/\tau)$ and we change (11) to the form

$$v_y / u_0 \leq k^{2/3} / (1 + t/\tau). \quad (12)$$

The maximum value of k at which (7) and (8) are satisfied can be evaluated if we assign the error of v_y . For example,

$$\frac{\Delta v_y}{v_y} = \frac{b \ln(1 + t/\tau) - \frac{1-k}{1+k} b \ln[1 + (1+k)t/\tau]}{b \ln(1 + t/\tau)} \leq 0.1,$$

from which it follows that

$$[1 + (1+k)t/\tau](1-k)/(1+k) \geq (1 + t/\tau)^{0.9}. \quad (13)$$

Thus, if conditions (12) and (13) are satisfied, then the maximum rate of rise of the particles under the influence of the Magnus effect v_{yM} can be determined from Eq. (9). Meanwhile, the maximum rate of rise due to elastic reflection from the obstacle v_{y0} does not exceed v_0 .

Simple calculations show that $v_{yM}/v_{y0} > 1$ at $C_d \sim 0.7$ beginning with $t \geq 0.2\tau$, while $v_{yM}/v_{y0} > 4$ at $t \sim \tau$, i.e., the Magnus force should exert a significant effect on the dynamics of ascent of the disperse phase.

By integrating (9), we obtain an expression for the height of ascent of the particles in relation to the time of interaction with the gas flow

$$h(t) = b\tau\{1 + (1 + t/\tau)[\ln(1 + t/\tau) - 1]\}. \quad (14)$$

This expression is valid for the tests shown in Fig. 2, since conditions (12) and (13) are not violated ($v_y = dh_+/dt < 60$ m/sec at $t \leq 2\tau$, $u_0 = 660$ m/sec, $\rho_g = 4.3$ kg/m³, $C_d \sim 0.7$, $d \sim 200$ μ m, $\rho = 1.2 \cdot 10^3$ kg/m³, $\tau \sim 160$ μ sec). Comparison of the experimental data on $h_+(t)$ and data calculated from (14) for $h(t)$ shows that Eq. (14) qualitatively reflects the character of the change in the height of particle ascent over time. Satisfactory quantitative agreement between the values of $h_+(t)$ determined experimentally and by calculation is seen at $b = 50$ m/sec (see Fig. 2, I, II).

Let us evaluate v_0 and the corresponding frequency of rotation $f = \omega/2\pi$ necessary to ensure the particle ascent observed experimentally. It is easily determined from Eq. (8) that the parameter $b = 50$ m/sec corresponds to $v_0 \geq 8$ m/sec and $f \sim 10^4$ sec⁻¹. In our opinion, these values are quite realistic. For example, the rotation of a particle with $d \sim 200$ μ m at a frequency $f \sim 2 \cdot 10^3$ sec⁻¹ was observed experimentally in [11] in the discharge of a two-phase jet from a tube at the velocity ~ 28 m/sec.

Thus, the completed studies make it possible to propose that particle collision plays an important role in the mechanism of formation of a two-phase layer behind a shock wave ($M = 2-3$, $p = 1$ atm) sliding over the surface of a layer of spherical particles of the size 50-500 μ m and density 1.2-8.6 g/cm³. Such collisions lead to rotation of the particles and, thus, to manifestation of the Magnus effect. It was shown that the action of the Magnus effect can satisfactorily explain the dynamics of ascent of spherical particles in the above range of parameters.

LITERATURE CITED

1. A. A. Borisov, B. E. Gel'fand, and S. A. Tsyganov, 1st Intern. Colloquium on Explosibility of Industrial Dusts, Baranow, Part 2 (1984).
2. J. H. Gerrard, Br. J. Appl. Phys., 14, No. 4, 186 (1963).
3. B. Fletcher, J. Phys. D, 9, No. 2, 197 (1976).
4. W. Mezkirch and K. Bracht, Intern. J. Multiphase Flow, 4, No. 1, 89 (1978).
5. T. Suzuki and T. Adashi, 13th Intern. Symp. Space Technol., Tokyo (1983).
6. V. P. Korobeinikov, V. V. Markov, and I. S. Men'shov, 1st Intern. Colloquium on Explosibility of Industrial Dusts. Baranow, Part 1 (1984).
7. V. M. Boiko, A. M. Papyrin, and S. V. Poplavskii, 3rd Intern. School on Explosibility of Industrial Dusts, Turawa, Part 2 (1982).
8. V. M. Boiko, A. A. Karnaukhov, V. F. Kosarev, et al., Zh. Prikl. Mekh. Tekh. Fiz., No. 3, 64 (1982).
9. V. M. Boiko, T. P. Gavrilenko, A. N. Papyrin, et al., 19, No. 3, 126 (1983).
10. M. A. Gol'dshtik and V. N. Sorokin, Zh. Prikl. Mekh. Tekh. Fiz., No. 6, 149 (1968).
11. A. A. Chernov, Dokl. Akad. Nauk SSSR, 105, No. 6, 1170 (1955).